Supporting information

Breaking the Chlorine and Oxygen Evolution Scaling Relation via the Selective Shielding Effect of Oxophilic Ti Sites

Ruiting Liu,[a] Jiachen Wang,[b] Yan Zhang,[b,c*] Lu Wang,[d] Jingjing Zhan,[a*] and Baoxue Zhou[c*]

[a.] School of Chemical Engineering, Ocean and Life, Dalian University of Technology, Dalian, 116024, China.

[b.] Key Laboratory of Industrial Ecology and Environmental Engineering (Ministry of Education, China), School of Environmental Science and Technology, Dalian University of Technology, Dalian, 116024, China.

[c.] School of Environmental Science and Engineering, Key Laboratory of Thin Film and Microfabrication Technology (Ministry of Education), Shanghai Jiao Tong University, Shanghai 200240, China.

[d.] School of Civil Engineering, Key Laboratory of Water Supply & Sewage Engineering of Ministry of Housing and Urban-rural Development, Chang'an University, Xi'an 710061, China.

1. Methods

1.1 Synthesis of $Co(OH)_2$/FTO nanowires

$Co(OH)_2$ nanowires were fabricated based on previous reports. Briefly, 5 mmol of cobalt nitrate, 10 mmol of ammonium fluoride and 25 mmol of urea were mixed in deionized water of 60 mL by magnetic stirring to form a pink transparent solution. The mixture was then transferred to a 100 mL Teflon-lined stainless-steel autoclave, and a piece of FTO substrate (2×5 cm^2) with the conductive facet facing down was immersed into it. After maintaining at 120℃ for 4 h, the autoclave was cooled down to room temperature. The as-obtained material was washed with deionized water and ethanol for several times to form $Co(OH)_2$/FTO nanowires.

1.2 Preparation of Co_3O_4/TiO_2 core-shell nanowires

Initially, the as-prepared $Co(OH)_2$ nanowires were immersed in 100 mL of ethanol. Subsequently, 1.0 mL of aqueous ammonia (28 wt %) was added dropwise to the solution for 30 min. 0.5 mL of TBOT ($C_{16}H_{36}O_4Ti$) was added as a precursor for the growth of TiO_2 on $Co(OH)_2$ nanowires, and the reaction mixture was maintained at 35 °C for 9 h to accelerate the hydrolysis of TBOT. After washing with deionized water, the synthesized $Co(OH)_2/TiO_2$ NWs were treated by 30 mL of 2 M NaOH at 30 °C for 5 h and 30 mL of 0.1 M HCl at room temperature for 5 min. The TiO_2 shell was converted into titanate, which protected $Co(OH)_2$ during these reactions. Finally, $Co(OH)_2$/titanate was annealed at 500°C for 2 h under N_2 atmosphere to yield Co_3O_4/TiO_2 NWs.

1.3 Synthesis of RuO_2 film on FTO

RuO_2 electrode was assembled through carefully loading 8.0 mM $RuCl_3$ solution ($V_{deionized\ water}$:$V_{ethanol}$=1:19) onto a FTO substrate followed by drying at 80℃ for 10 min. This process was repeated to achieve a deposition amount of 0.3 mg cm^{-2} (calculated according to the amount of formed RuO_2). In the end, the electrode was annealed at 350℃ for 2 hours to generate RuO_2 film.

1.4 Characterizations

The X-ray powder diffraction (XRD) patterns were recorded using a Rigaku D-Max B diffractometer with Cu Kα radiation (λ = 0.15418 nm). The morphological characterizations were collected by scanning electron microscopy (SEM, Zeiss SUPRA55-VP); besides, corresponding energy-dispersive X-ray spectroscopy (EDX) was equipped for elemental identification. The transmission electron microscopy (TEM) images of catalysts were taken on JEOL JEM-2010 high resolution transmission electron microscopes. The Raman spectra were obtained by a LabRam Aramis equipment (Horriba Jovin Yvon Inc., US). Chemical bonds between elements were observed on a Fourier transform infrared spectrometer (FTIR, Nicolet 6700) in the wave-number range of 400-4000 cm^{-1}. X-ray photoelectron spectroscopy (XPS) analyses were carried out to determine elements and valence states on an Omicron EA125 spectrometer, with all XPS spectra energy-calibrated by hydrocarbon peak at 284.8 eV.

1.5 Electrochemical measurements

All the electrochemical measurements were conducted in a conventional three-electrode system controlled by an electrochemical workstation (CHI 660D, Shanghai Chenhua) at room temperature. The test was performed using prepared catalyst, Pt plate, and Ag/AgCl electrode (saturated KCl) as the working electrode, counter electrode, and reference electrode, respectively. Polarization curves were obtained with linear sweep voltametric (LSV) in the potential range of 0.5 to 2.0 V *(*vs. Ag/AgCl*)* at a scan rate of 20 mV S^{-1} NaCl aqueous solution. The onset potential was determined using the tangent intersection method. Specifically, a tangent line was drawn along the linear region of maximum slope for the faradaic current in the LSV curve. The intersection of this tangent line with the baseline current was defined as the onset potential.

Electrochemical impedance spectroscopy (EIS) was performed over a frequency range of 10^5 to 10^{-1} Hz at open circuit potential of 1.0 V, and the results were processed with a ZSim Demo software. The electrochemical active surface area (ECSA) was determined by electrochemical double-layer capacitance (C_{dl}) measurements. The C_{dl}

was determined by CV measurements in a range without Faraday current by plotting the half of the difference value in current density between anodic and cathodic sweeps (Δj/2) at a fixed potential and fitting the slope value. All the potential measured were converted into reversible hydrogen electrode (RHE) reference scale by using the following equation:

$$E_{RHE} = E_{Ag/AgCl} + 0.197V + 0.0591 \times pH \quad (1)$$

where the pH was measured by pH meter. Pure argon gas was purged into the electrolyte for 30 min to remove any dissolved oxygen gas before the electrochemical performance test. The equilibrium potential for CER under the experimental condition could be influenced by temperature based on the Nernst equation[16]. In this work, the CER equilibrium potential is considered as E_{CER}=1.36V vs RHE according to previously published research.

The Cl_2 selectivity of the electrocatalysts was analyzed by iodometric titration method and calculated via the equation below:

$$Cl_2(\%) = 100 \times \frac{experimental\ yield}{theoretical\ yield} = \frac{\frac{0.01M \times V_{Na_2S_2O_3}}{2}}{\frac{i \times t}{2F}}$$

(2) where i, t, F, $V_{Na2S2O3}$ is the current, time, faraday constant (96,485 C mol^{-1}), and the volume of $Na_2S_2O_3$ solution, respectively. During the iodometric titration testing, chronoamperometry was conducted at 10 mA cm^{-2} for 200 s. After that, 5 mL of the anodic electrolyte was collected and immediately transferred into a 25 mL flask containing a large excess of KI. Subsequently, 0.01mol L^{-1} $Na_2S_2O_3$ was utilized to titrate the solution by using starch as the indicator.

The turnover frequency (TOF) values can be obtained by using the following equation:

$$TOF = \frac{J \times A}{2 \times F \times m} \quad (3)$$

where J, A, F, m represents the obtained current density at varied overpotentials, electrode

area, faraday constant (96,485C mol^{-1}), and the number of moles of active sites, respectively.

1.6 Ammonia oxidation

The electrolysis experiments were conducted in an undivided electrochemical cell containing 50 mL of synthetic wastewater. The wastewater composition was 30 mg L^{-1} NH_3-N, 0.05 mol L^{-1} Na_2SO_4, and 30 mM NaCl, with the initial pH adjusted to 3.0. A standard three-electrode system was utilized, with Co_3O_4/TiO_2 as the working electrode, a Pt mesh as the counter electrode, and an Ag/AgCl electrode as the reference electrode. The conversion process was carried out by applying a constant potential of 1.8 V (vs. Ag/AgCl). Liquid samples (1.0 mL) were periodically extracted at predetermined intervals for the analysis of ammonia and nitrate concentrations.

The concentration of NH_3 was determined using the salicylic acid method. Specifically, the electrolyte was collected from the cathode cell. 2.0 mL of sample was mixed with 2.0 mL of 1.0 M NaOH solution containing 5 wt% salicylic acid and 5 wt% sodium citrates. 1.0 mL of 0.05 M NaClO and 0.2 mL of $C_5FeN_6Na_2O$ solution (1 wt%) were added to the mixture component and shaken well. After stewing for 1 h, UV-vis measurements were performed with the range from 500 to 800 nm and recorded the absorbance at the wavelength of 655 nm. We have provided a detailed method in the supporting materials.

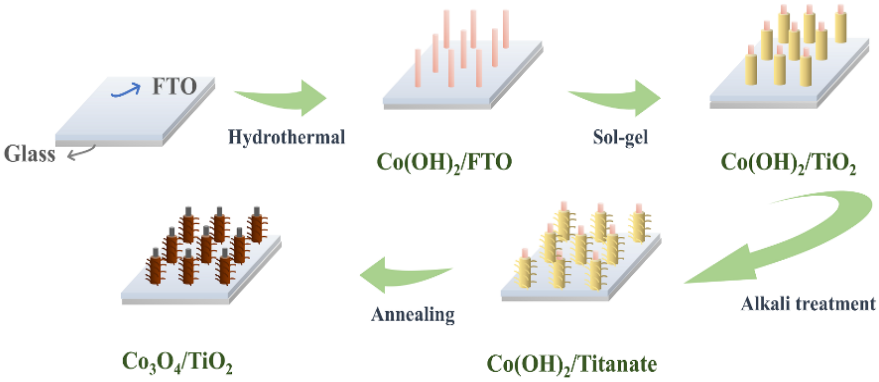

Fig. S1 Schematic illustration of the synthesis of Co_3O_4/TiO_2 core-shell NWs.

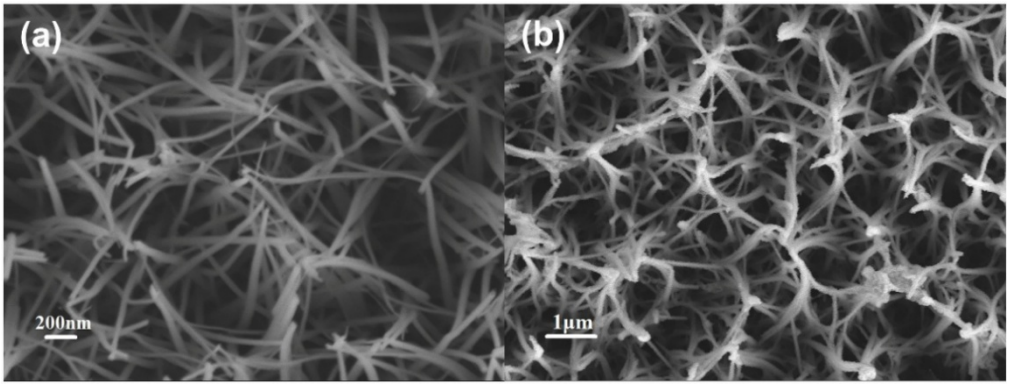

Fig. S2 The SEM images of (a) $Co(OH)_2$ and (b) Co_3O_4.

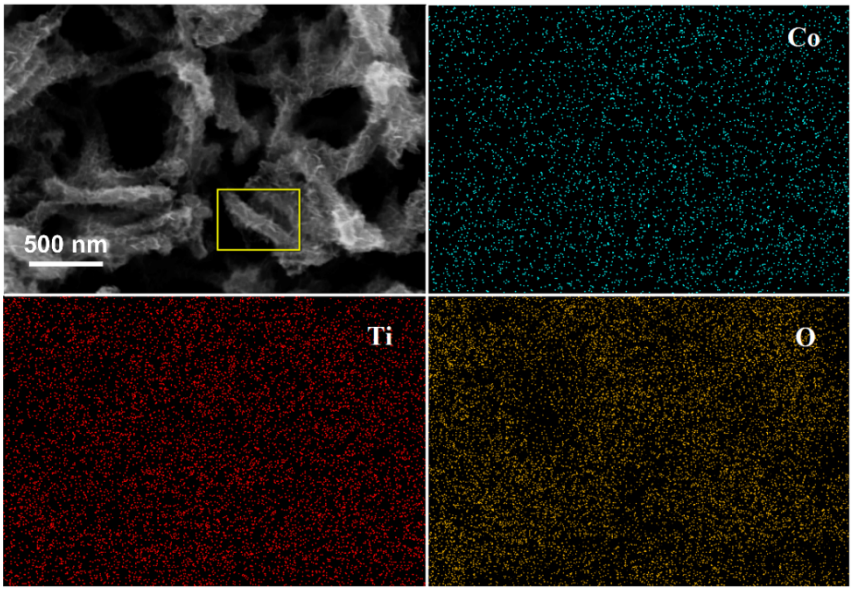

Fig.S3 EDS mapping of Co_3O_4/TiO_2 by SEM.

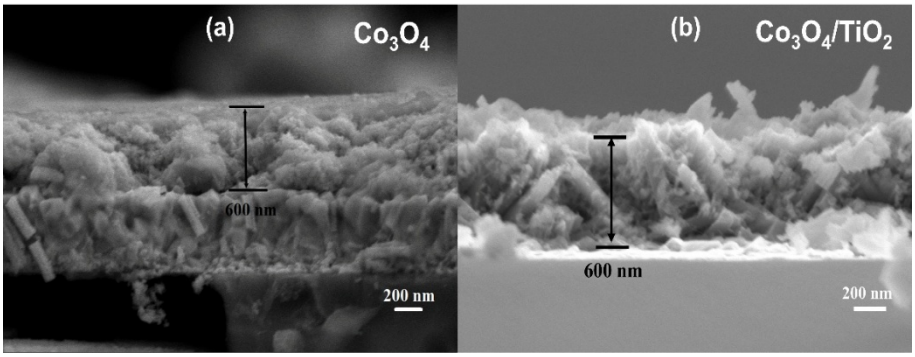

Fig.S4 The cross-sectional images of Co_3O_4 and Co_3O_4/TiO_2 by SEM.

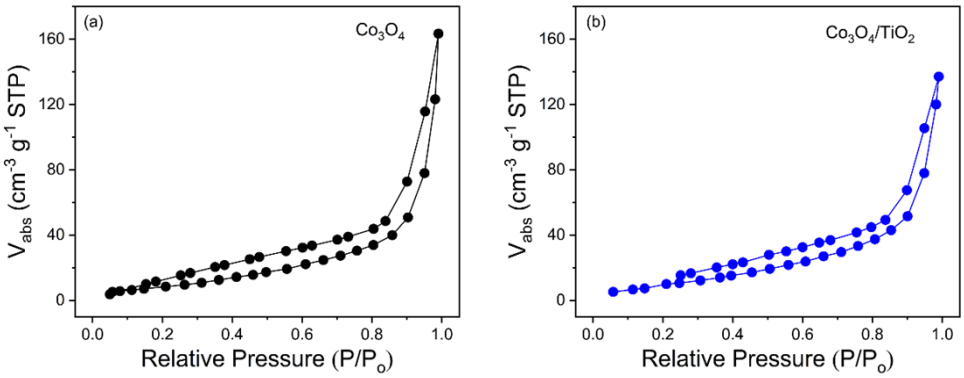

Fig.S5 Nitrogen adsorption/desorption isotherms of Co_3O_4 and Co_3O4/TiO_2.

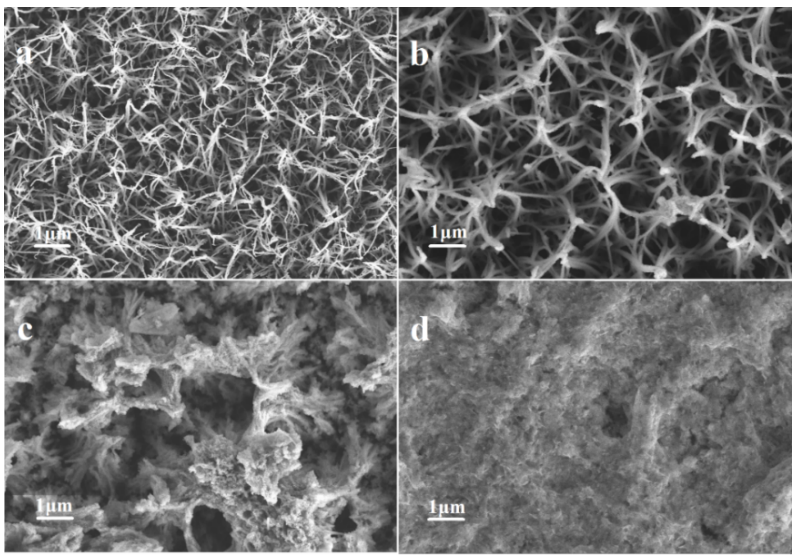

Fig.S6 SEM images of Co_3O_4/TiO_2 at controlled deposition time. (a) 3 h, (b) 6 h, (c) 9 h and (d)12 h.

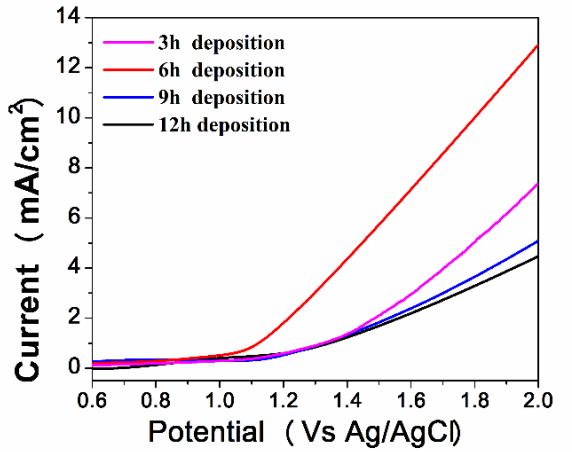

Fig.S7 CER polarization curves of Co_3O_4/TiO_2 NWs at different deposition time.

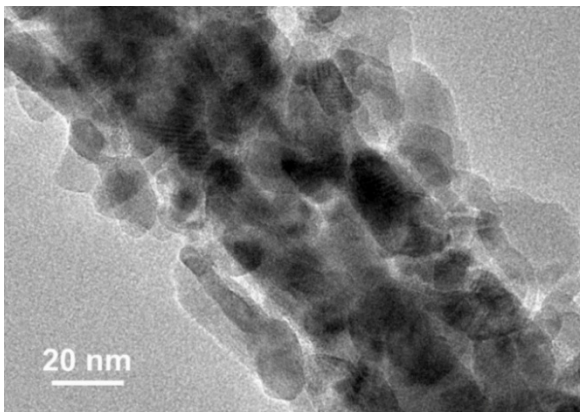

Fig.S8 TEM views of Co_3O_4/TiO_2 NWs.

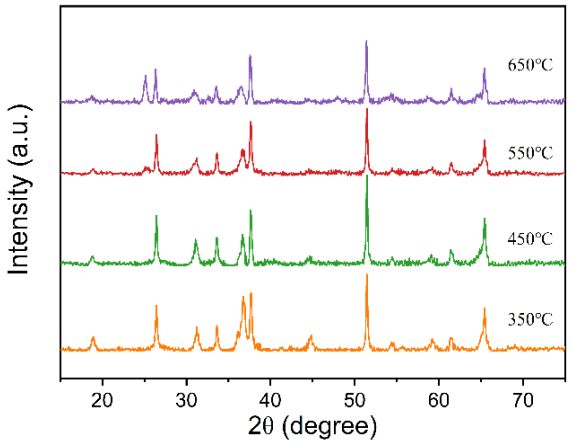

Fig.S9 XRD patterns of Co_3O_4/TiO_2 NWs under different annealing temperatures.

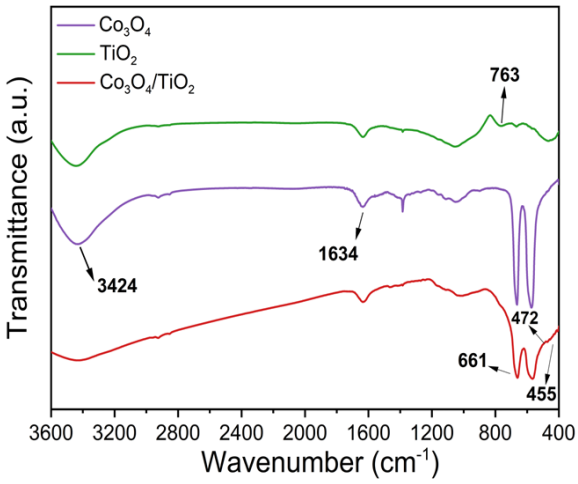

Fig.S10 FTIR spectra of as-prepared materials.

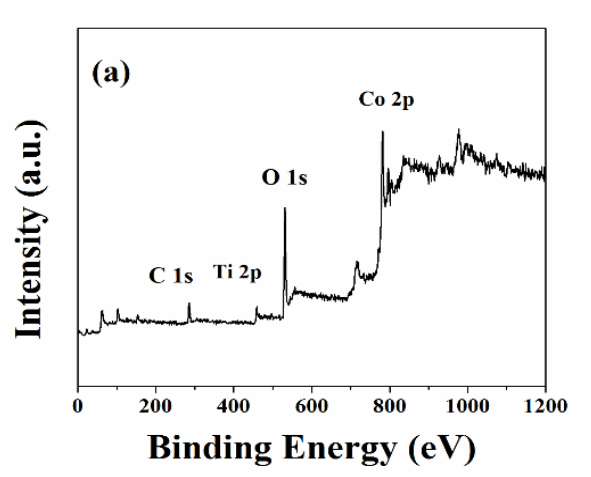

Fig.S11 XPS survey spectrum of Co_3O_4/TiO_2.

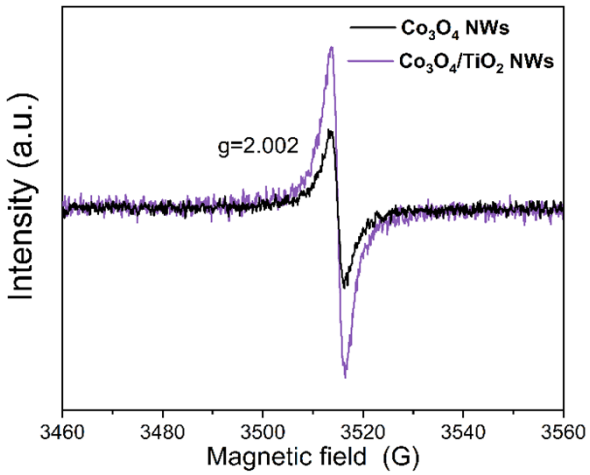

Fig.S12 EPR image of Co_3O_4/TiO_2 NWs.

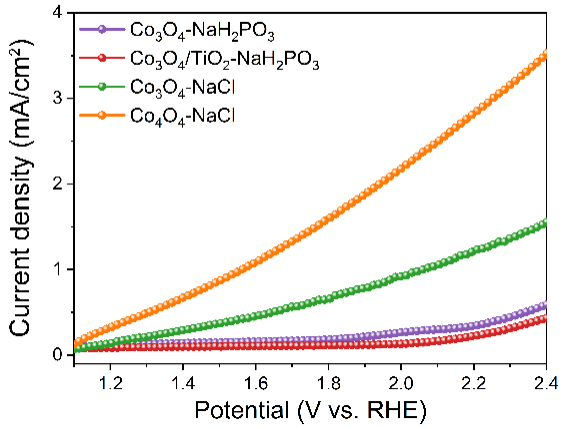

Fig.S13 LSV curves of Co_3O_4/TiO_2 and Co_3O_4 anodes in NaCl and NaH_2PO_4 solutions.

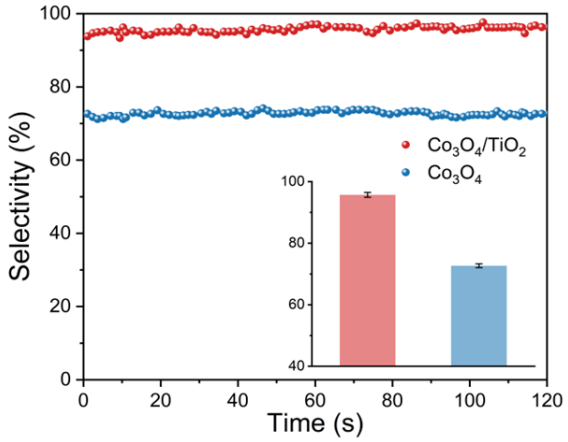

Fig.S14 FE of the prepared Co_3O_4 and Co_3O_4/TiO_2.

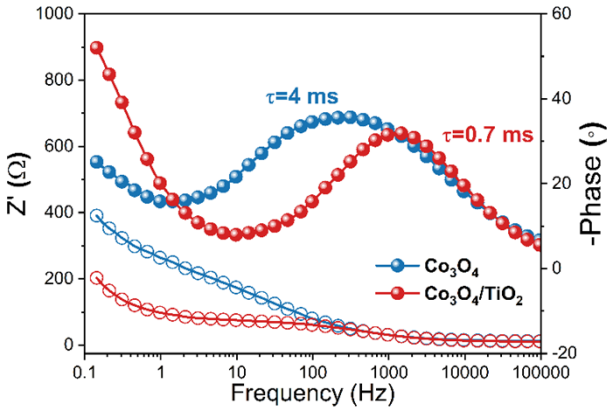

Fig.S15 The Bode format of the impedance spectra.

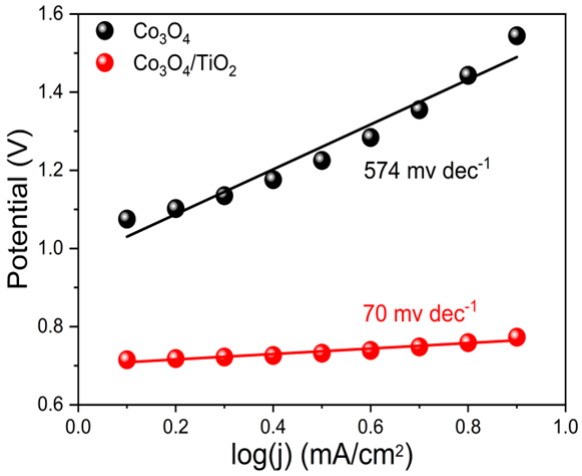

Fig.S16 Tafel plots of the Co_3O_4/TiO_2 and Co_3O_4.

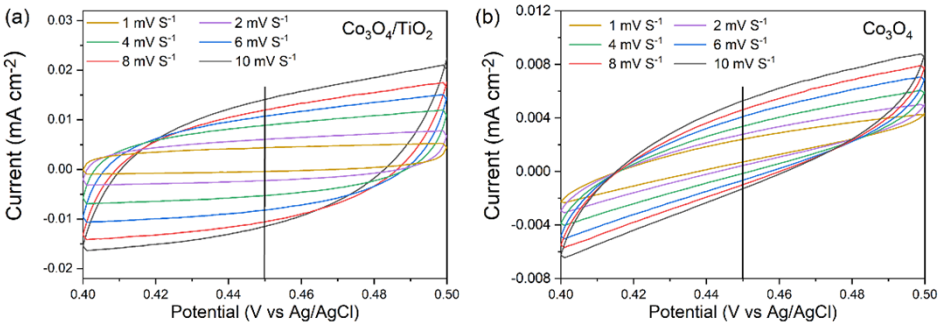

Fig. S17 CV curves of (a) Co_3O_4/TiO_2 and (b) Co_3O_4 in the double layer region at different scan rates.

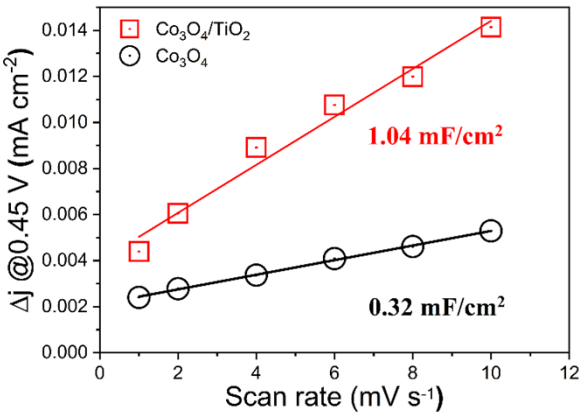

Fig. S18 ECSA analysis of Co_3O_4/TiO_2 and Co_3O_4.

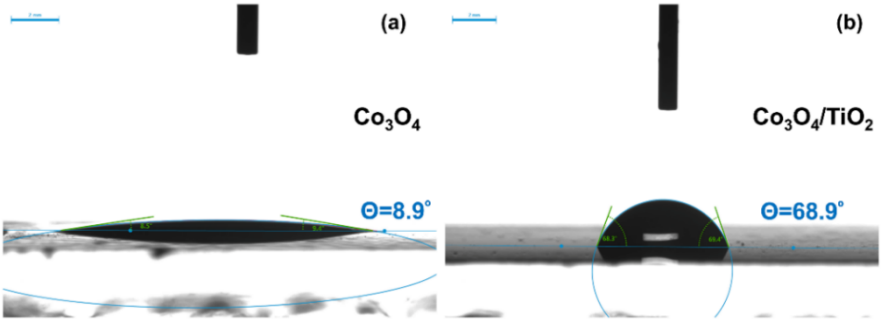

Fig. S19 Water contact angle of Co_3O_4/TiO_2 and Co_3O_4.

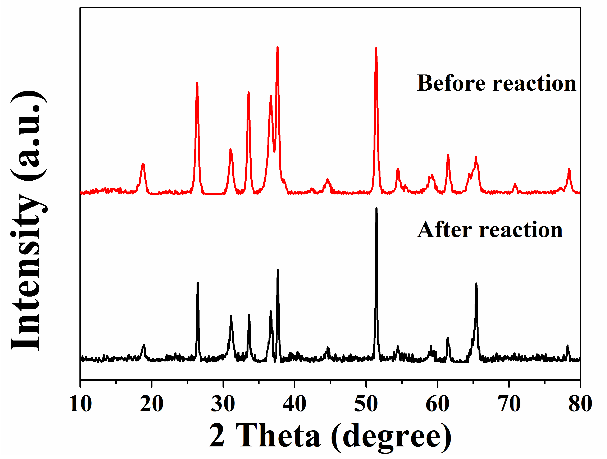

Fig. S20 XRD patterns of Co_3O_4/TiO_2 anode before and after reaction.

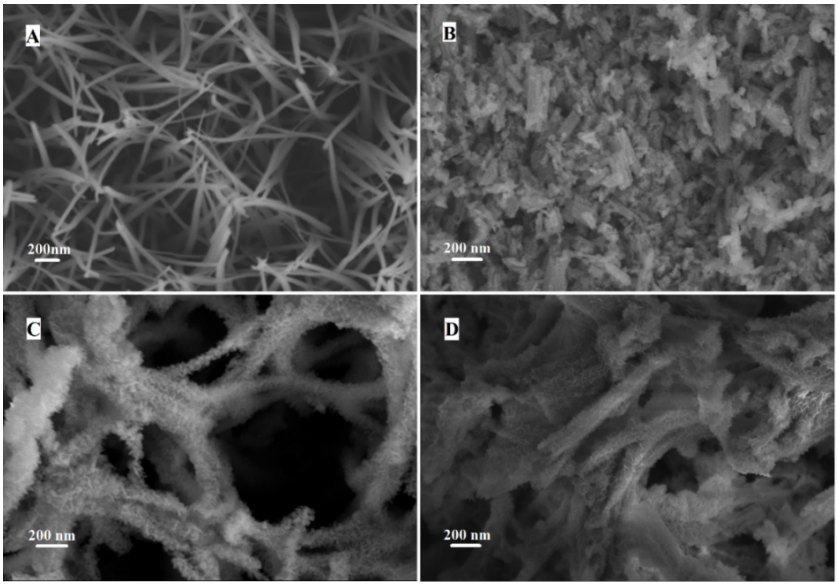

Fig. S21 SEM images of (a) fresh Co_3O_4, (b) used Co_3O_4 in acidic solution (pH=3). (c) fresh Co_3O_4/TiO_2, (d) used Co_3O_4/TiO_2 in acidic solution (pH=3).

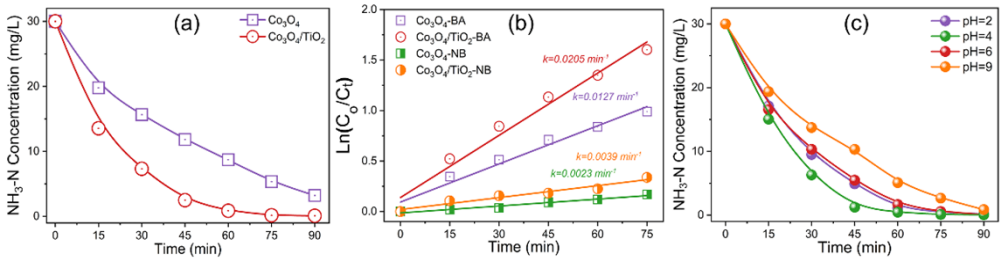

Fig. S22 (a) Ammonia removal versus time on different anodes. (b) Degradation performances in the system at different applied potential. (c) Degradation performances at varied initial pH.

Table.S1 Parameters determined from electrochemical measurements

Sample	R_s (Ω)	R_{ct} (Ω)	R_{ad} (Ω)
Co_3O_4	10.8	254.6	92.1
Co_3O_4/TiO_2	10.2	57.1	67.9